 

*EXTREME LASER RADIATION: PHYSICS AND FUNDAMENTAL APPLICATIONS* https://doi.org/10.1070/QEL16307

# 100 J-level pulse compression for peak power enhancement

S.Yu. Mironov, J. Wheeler, R. Gonin, G. Cojocaru, R. Ungureanu, R. Banici, M. Serbanescu, R. Dabu, G. Mourou, E.A. Khazanov

*Abstract.* **A possibility of using self-phase modulation and cascaded quadratic nonlinearity effects for the enhancement of the temporal intensity profile is analysed theoretically in application to petawatt pulses at a kJ energy level. Preliminary experiments at a petawatt CETAL laser facility demonstrate the reduction of a pulse duration from 46 fs down to 29 fs by using the self-phase modulation effect and consequent spectral phase correction. These efficient methods offer an opportunity to economically enhance existing laser facility intensities and offer a broader range of high-intensity physics to become more readily attainable.**

***Keywords:*** *compression of femtosecond pulses, petawatt pulses, self-phase modulation, second harmonic.*

## 1. Introduction

Enhancing the peak intensity of high-energy pulsed laser systems typically involves a large investment in upgrades and additional amplification stages with the goal of increasing the useful energy contained within the pulse. Another option is to further compress the existing pulse energy within reduced time duration. The motivation for an efficient method to post-compress J-level laser systems is multifold. The initial, most straightforward reason, especially for the highest energy laser systems with durations greater than 50 fs, is for an inexpensive peak intensity enhancement without the need for large investments to extend beyond current pulse energies. This suggests that the peak power of current petawatt, or near-petawatt, systems have the capacity to be extended up to and beyond 7–10 PW, which makes possible previously inaccessible experiments such as the study of nonlinear properties of vacuum, generation of electron–positron pairs and efficient generation of optical harmonics.

The brightest examples of lasers with a kilojoule energy level are the Texas petawatt laser [1] and the PETAL laser facility in Bordeaux, France [2, 3]. Both systems utilise chirped pulse amplification (CPA) in neodymium doped laser glass. To date, the record peak intensity at $10^{22}$ W cm$^{-2}$ is set by the HERCULES laser in Michigan, which becomes possible by using a high-energy, short-pulse scheme (9 J, 30 fs) with tight focusing [4]. The post-compression of existing laser systems that contain a greater pulse energy toward similar short pulse durations will allow for even greater peak intensities in the near future.

In this paper, we analyse the possibility of peak power enhancement of long-pulse laser systems taking as an example the PETAL laser facility. The feasibility of three techniques is considered: self-phase modulation (SPM) [5, 6], second harmonic generation (SHG) and self-compression through a cascaded quadratic nonlinearity in a KDP crystal [cascaded self-compression (CSC)]. The PETAL laser has the following output radiation parameters: transverse beam size of ~400 mm, centre wavelength of 1053 nm and pulse duration shorter than 0.5 ps. The laser pulse peak power is ~2 PW.

After discussion of the compression methods, the results of preliminary experiments conducted at the petawatt CETAL laser facility on the SPM compression technique are presented.

## 2. Techniques for peak power enhancement

### 2.1. Self-phase modulation

One of the most promising ways of increasing peak power is a method based on the self-phase modulation effect. During the propagation of intense optical pulses in media with cubic nonlinearity, their parameters are modified, i.e. the spectrum is broadened and the phase is modulated. Correction of the quadratic component of the spectral phase by means of chirped mirrors reduces the duration by several times, thereby increasing the peak power [6].

Evolution of the parameters of a laser pulse propagating in a medium with cubic nonlinearity is described by the equation in the second approximation of the dispersion theory:

**S.Yu. Mironov, E.A. Khazanov** Institute of Applied Physics, Russian Academy of Sciences, ul. Ul'yanova 46, 603950 Nizhnii Novgorod, Russia; e-mail: sergey.mironov@mail.ru;
**J. Wheeler** IZEST, École Polytechnique, Route de Saclay, 91128 Palaiseau cedex, France; Horia Hulubei National Institute of Physics and Nuclear Engineering, Extreme Light Infrastructure – Nuclear Physics, str. Reactorului 30, 077125 Magurele, Bucharest, Romania;
**R. Gonin** IZEST, École Polytechnique, Route de Saclay, 91128 Palaiseau cedex, France; Université Paris-Sud, 15 Rue Georges Clemenceau, 91400 Orsay, France;
**G. Cojocaru, R. Ungureanu** CETAL, National Institute for Laser, Plasma and Radiation Physics, Atomistilor str. 409, 077125 Magurele, Bucharest, Romania; Faculty of Physics, University of Bucharest, Atomistilor str. 405, 077125 Magurele, Bucharest, Romania;
**R. Banici** National Institute for Laser, Plasma and Radiation Physics, Atomistilor str. 409, 077125 Magurele, Bucharest, Romania;
**M. Serbanescu** CETAL, National Institute for Laser, Plasma and Radiation Physics, Atomistilor str. 409, 077125 Magurele, Bucharest, Romania;
**R. Dabu** Horia Hulubei National Institute of Physics and Nuclear Engineering, Extreme Light Infrastructure – Nuclear Physics, str. Reactorului 30, 077125 Magurele, Bucharest, Romania;
**G. Mourou** IZEST, École Polytechnique, Route de Saclay, 91128 Palaiseau cedex, France

Received 6 February 2017
*Kvantovaya Elektronika* **47** (3) 173–178 (2017)
Submitted in English

$$\frac{\partial A}{\partial z}+\frac{1}{u}\frac{\partial A}{\partial t}-\mathrm{i}\frac{k_2}{2}\frac{\partial^2 A}{\partial t^2}+\mathrm{i}\gamma_1|A|^2A$$

$$+\frac{3\pi\chi^{(3)}}{nc}\frac{\partial}{\partial t}(|A|^2A)=0, \qquad (1)$$

where $A(t-z/u, z)$ is the complex amplitude of the field; $\gamma_1 = 3\pi k_0\chi^{(3)}/(2n_0^2)$; $\chi^{(3)}$ is the nonlinear susceptibility; $k_0$ is the wave vector; $n_0$ is the linear part of the refractive index; $t$ is the time; $z$ is the longitudinal propagation coordinate; $k_2 = \partial^2 k/\partial\omega^2|_{\omega_0}$ is the group velocity dispersion (GVD) parameter; and $u$ is the group velocity. Equation (1) may be solved numerically using the split-step method [7] in combination with difference schemes. We assume that the spectral phase is managed by dispersive mirrors that correct the quadratic phase dependence of the frequency. Mathematically, the operation is described by

$$A_c(t)=F^{-1}\left[\exp\left(-\frac{\mathrm{i}\alpha\omega^2}{2}\right)F(A_{\mathrm{out}}(t,L))\right]. \qquad (2)$$

Here, $F$ and $F^{-1}$ are the operators of the direct and inverse Fourier transform; $\alpha$ is the group delay dispersion (GDD) parameter of the phase corrector; $\omega$ is the centre frequency offset; and $A_{\mathrm{out}}(t, z = L)$ is the field amplitude at the nonlinear medium output.

Spectral broadening during the propagation of intense radiation through a medium with cubic nonlinearity is determined by both the initial pulse phase and the accumulated nonlinear phase ($B$-integral) $B = \gamma_1|A_{\max}|^2L$, where $L$ is the thickness of the nonlinear medium [8]. For $B < 1$ rad, the spectral change is insignificant and this case is of no interest for the solution of the problem on peak power enhancement. It is known [9] that for $B > 2$ rad, small-scale self-focusing may develop, leading to appreciable modulation of the transverse distribution of the beam and, finally, to destruction of the nonlinear element. However, for intense ($\sim$TW cm$^{-2}$) radiation there is a simple method for suppressing this undesirable effect using a beam free path in vacuum for filtering spatial harmonic perturbations that are most amplified [10].

Currently, plane-parallel plates made of optical glass, fused silica as well as transparent polymers with a thickness of $\sim$1 mm at an aperture of $\sim$400 mm are available. Moreover, the thickness of polymers can be significantly less than 1 mm with an unlimited aperture for the observed laser beams [11].

Results of numerical simulation of spectrum broadening in a sample of 3-mm-thick fused silica are presented in Fig. 1. The following parameters of the material were used: cubic nonlinearity of fused silica $2.43\times10^{-7}$ cm$^2$ GW$^{-1}$ [12] and parameter of group velocity dispersion $k_2 = 20.1$ fs$^2$ mm$^{-1}$. We assume that at the input of the nonlinear medium the Fourier transform-limited pulse has a Gaussian shape with a duration of 500 fs (FWHM intensity), a pulse energy of 1 kJ and a transverse beam size of 400 mm. Assuming that the transverse intensity distribution in space is plane, the peak intensity of the radiation for the above mentioned parameters will be 1.5 TW cm$^{-2}$. In the course of pulse propagation in a sample of fused silica the pulse accumulates a $B$-integral equal to 6.5 rad.

The intensity distributions of the spectra of the initial pulse and of the pulse transmitted through the silica nonlinear element are plotted in Fig. 1a. Cubic nonlinearity ($B$-integral in particular) leads to spectrum broadening and modulation. At the same time, the difference between the temporal intensity distribution before and after the nonlinear element is insignificant (Figs 1b and 1c). By correcting the quadratic phase component of output radiation, the pulse duration may be reduced down to 108 fs and the peak intensity may be increased up to 6 TW cm$^{-2}$ in the unfocused beam. In this case, the GDD parameter that gives the greatest peak power enhancement is $\alpha = -10^4$ fs$^2$. Such a phase correction may be realised in experiments using commercial chirped mirrors with anomalous group velocity dispersion.

It is important to note that this method increases the temporal contrast of radiation in the near region of the main pulse (Fig. 1c), the contrast in the far region of the main maximum remaining unchanged. It is well known that the tempo-

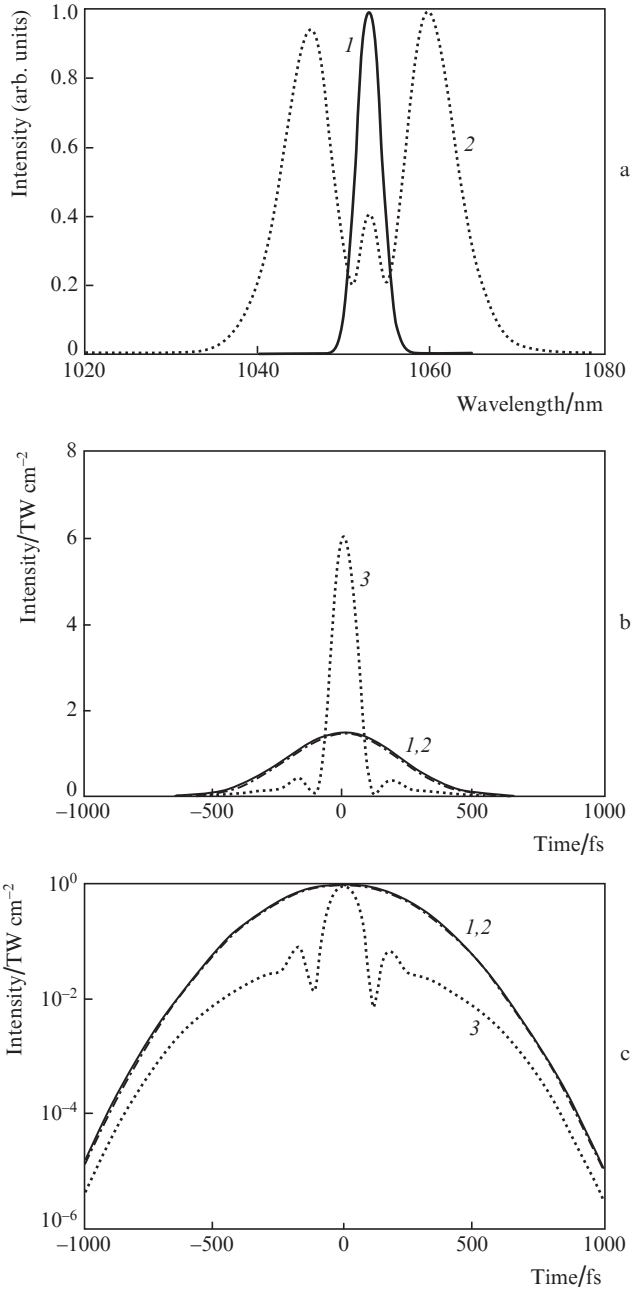


**Figure 1.** (a) Spectral intensity distributions and (b, c) time intensity profiles: (*1*) initial pulse, (*2*) at the nonlinear medium output, and (*3*) after correction of the quadratic component of the phase.

ral contrast in the far region may be increased significantly (by a power of two) by means of the second harmonic generation (SHG).

### 2.2. Second harmonic generation

The SHG of high-energy laser radiation results not only in a twofold decrease in the wavelength but also in a pronounced increase in the temporal contrast in the region far from the main pulse. A shorter wavelength allows for the reduction in the laser beam focus size, which leads to a corresponding enhancement of the peak intensity. The improvement in temporal contrast is due to both the intrinsic nonlinearity of the SHG process as well as to the fact that laser super-luminescence propagating outside the SHG angular band does not contribute to the conversion to the second harmonic radiation. Moreover, when SHG occurs along with the conditions of the cubic nonlinearity effect, it becomes possible to also reduce the pulse duration and to increase the peak power. We will show that the second harmonic pulse may have a higher peak power than the initial pulse of the fundamental harmonic, as well as an improved temporal contrast by about a power of two. Numerical simulations rely on the parameters for the PETAL laser facility given above.

A KDP crystal will be introduced as the nonlinear crystal in the calculations. This crystal has a number of merits: it may be grown with a transverse size up to 400 mm; the difference between group velocities of the fundamental and second harmonics is very small in this crystal ($1/u_1 - 1/u_2 = 3$ fs mm$^{-1}$ at $\lambda = 1053$ nm for an oo–e interaction). Another very important feature of this crystal worth noting is that the GVD parameter for an ordinary wave at 1053 nm is negative ($k_2 = -17.1$ fs$^2$ mm$^{-1}$), while the cubic susceptibility tensor is positive. Actually, this crystal may be also used in the regime of intensity self-compression of the pulse at the fundamental harmonic when the effects of cubic nonlinearity come into play [13]. This issue will be addressed elsewhere. The parameter $k_2$ for the second harmonic pulse is 71 fs$^2$ mm$^{-1}$.

The process of conversion to the second harmonic is described by a system of coupled equations [14, 15]:

$$\begin{aligned}
&\frac{\partial A_1}{\partial z} + \frac{1}{u_1}\frac{\partial A_1}{\partial t} - \frac{\mathrm{i}k_2^{(1)}}{2}\frac{\partial^2 A_1}{\partial t^2} = -\mathrm{i}\beta A_1 A_2 \exp(-\mathrm{i}\Delta k z) \\
&\quad - \mathrm{i}\gamma_{11}|A_1|^2 A_1 - \mathrm{i}\gamma_{12}|A_2|^2 A_1, \\
&\frac{\partial A_2}{\partial z} + \frac{1}{u_2}\frac{\partial A_2}{\partial t} - \frac{\mathrm{i}k_2^{(2)}}{2}\frac{\partial^2 A_1}{\partial t^2} = -\mathrm{i}\beta A_1^2 \exp(\mathrm{i}\Delta k z) \\
&\quad - \mathrm{i}\gamma_{21}|A_1|^2 A_2 - \mathrm{i}\gamma_{22}|A_2|^2 A_2,
\end{aligned} \tag{3}$$

where $A_1(t,z)$ and $A_2(t,z)$ are the field envelopes of the fundamental and second harmonics; $u_1$ and $u_2$ are the group velocities; $k_2^{(1,2)}$ are the parameters of the dispersion of group velocities of the fundamental and second harmonic; $\beta$ and $\gamma_{ij}$ $(i,j = 1,2)$ are the coefficients of nonlinear wave coupling; and $\Delta k = k_2 - 2k_1$ is the wave vector detuning. According to work [15], for the o–oe interaction the optimal conversion to the second harmonic occurs for the offset from the phase matching angle

$$\Delta\theta = \frac{\Delta n}{n_1^3 (n_1^{-2} - n_\mathrm{o}^{-2})} \sqrt{\frac{n_1^{-2} - n_\mathrm{o}^{-2}}{n_\mathrm{e}^{-2} - n_1^{-2}}}, \tag{4}$$

where $\Delta n = \lambda |A_{10}|^2 (2\gamma_{11} + 2\gamma_{12} - \gamma_{21} - \gamma_{22})/(8\pi)$; and $A_{10}$ is the amplitude of the field of the fundamental wave at the input of the nonlinear medium. The angular offset (4) allows one to compensate for the contribution of the nonlinear phase to the reduced conversion efficiency. For the given parameters, $\Delta\theta = -2.68$ mrad.

The dependence of the efficiency of conversion to the second harmonic on the thickness of a KDP nonlinear element is given in Fig. 2a. The values of the coefficients $\gamma_{ij}$ were borrowed from work [14], where their analytical forms were pre-

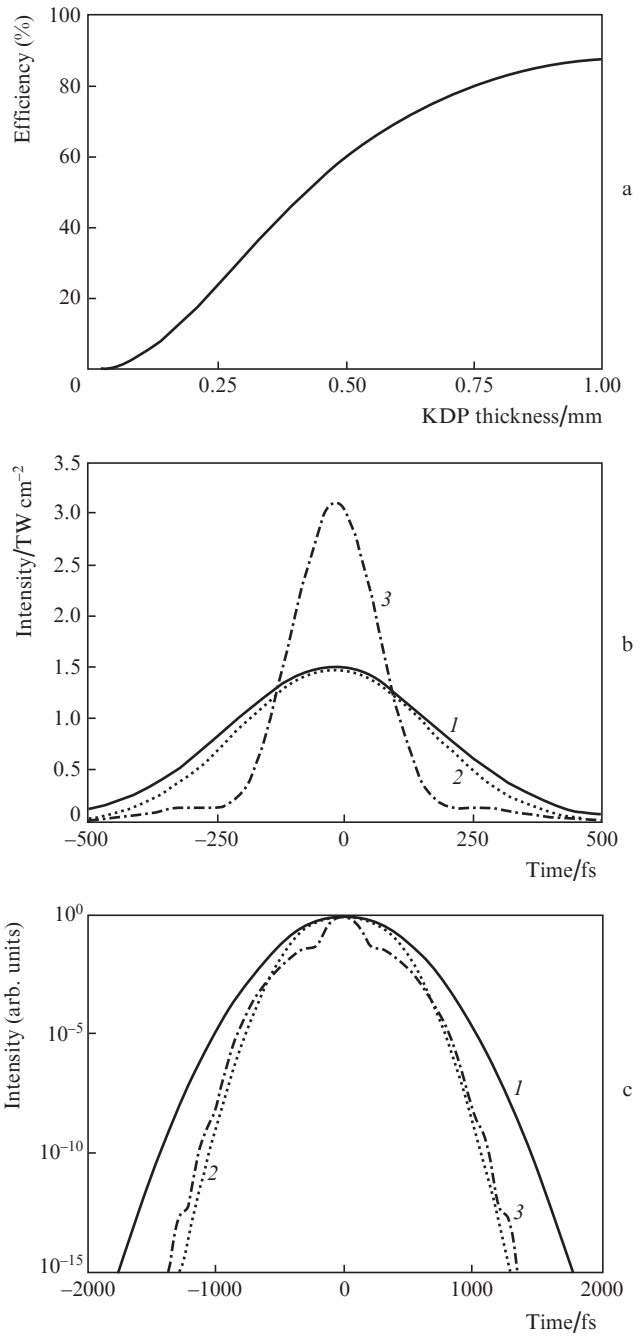


**Figure 2.** (a) Efficiency of energy conversion as a function of thickness of KDP nonlinear element and (b, c) temporal intensity profiles of (*1*) the initial pulse, (*2*) second harmonic pulse at the nonlinear medium output and (*3*) second harmonic pulse after correction of the quadratic component of the spectrum phase.

sented as a function of propagation angles in a crystal. According to the results of numerical simulations, the energy conversion efficiency is over 80%. The profiles of the initial radiation and the second harmonic pulse at the crystal output and after correction of the quadratic component of the spectrum phase at $\alpha = -1.77 \cdot 10^4$ fs$^2$ are presented in Figs 2b and 2c. The pulse duration of the second harmonic at the output of the nonlinear crystal is 460 fs, whereas the duration of the compressed pulse of the second harmonic is 200 fs. Conversion to the second harmonic and correction of the quadratic component of the spectrum phase enable enhancing the peak power approximately by a factor of 2.

According to Fig. 2c the time contrast of the second harmonic pulse is higher by approximately a power of two than the pulse of the fundamental harmonic. Note also that the correction of the quadratic component of the spectrum phase affects only the contrast close to the main peak of the second harmonic pulse and has no impact on the contrast of the pulse wings.

### 2.3. Self-compression in KDP crystal with using cascaded quadratic nonlinearity

The nonlinear interaction between the fundamental and second harmonic waves in the KDP crystal can also be used for peak power enhancement of the initial/fundamental laser pulse. The method is based on the implementation of a cascaded quadratic nonlinearity and has been successfully applied for the enhancement of the peak power in low-energy laser systems [16].

The value of an accumulated phase in the process of second harmonic generation depends on the value and sign of $\Delta k$ [see Eqn (3)]. Both can be easily varied in experiments by detuning the direction of propagation for the beam through the crystal. It should be noted that the phase obtained due to the cascaded quadratic nonlinearity is proportional to the intensity of the fundamental pulse as well as the phase obtained due to self-action effects. As a result, the cascaded quadratic nonlinearity can be used for compensation or magnification of cubic polarisation effects [16, 17].

For the same PETAL beam parameters presented above, Fig. 3 demonstrates the possibility of using a single KDP crystal for the efficient energy conversion to second harmonic and pulse recompression at the fundamental harmonic. Numerical simulations were performed for the above parameters of the PETAL laser facility. The cascaded quadratic nonlinearity permits the compression of an initial first-harmonic pulse from 500 fs down to 220 fs (see Fig. 3e), while insignificantly changing the contrast ratio of the temporal intensity (Fig. 3f).

## 3. Experimental study of SPM compression

Initial studies of the nonlinear interaction of a short, high-energy pulse have been conducted on the petawatt CETAL laser located at the INFLPR in Magurele-Bucharest, Romania. This preliminary work is carried out using the frontend of the 1 PW laser system, which provided a pulse of 200 mJ, 50 fs at a repetition rate of 10 Hz. To achieve the properties of the full PW beam the size of the beam is reduced to an area of 1 cm$^2$ by using a reducing telescope based on large-diameter silver and small-diameter dielectric coated spherical mirrors (see Fig. 4). An upper limit for the pulse fluence was placed at 120 mJ cm$^{-2}$ in order to stay below the damage threshold for the coatings of the dispersive controlled, chirped mirrors. Any large variations in the beam spatial profile led to a damage of the smaller re-collimating spherical mirror at these intensities. In this connection, for the problem in question, a uniform pulse intensity profile is of importance not only for

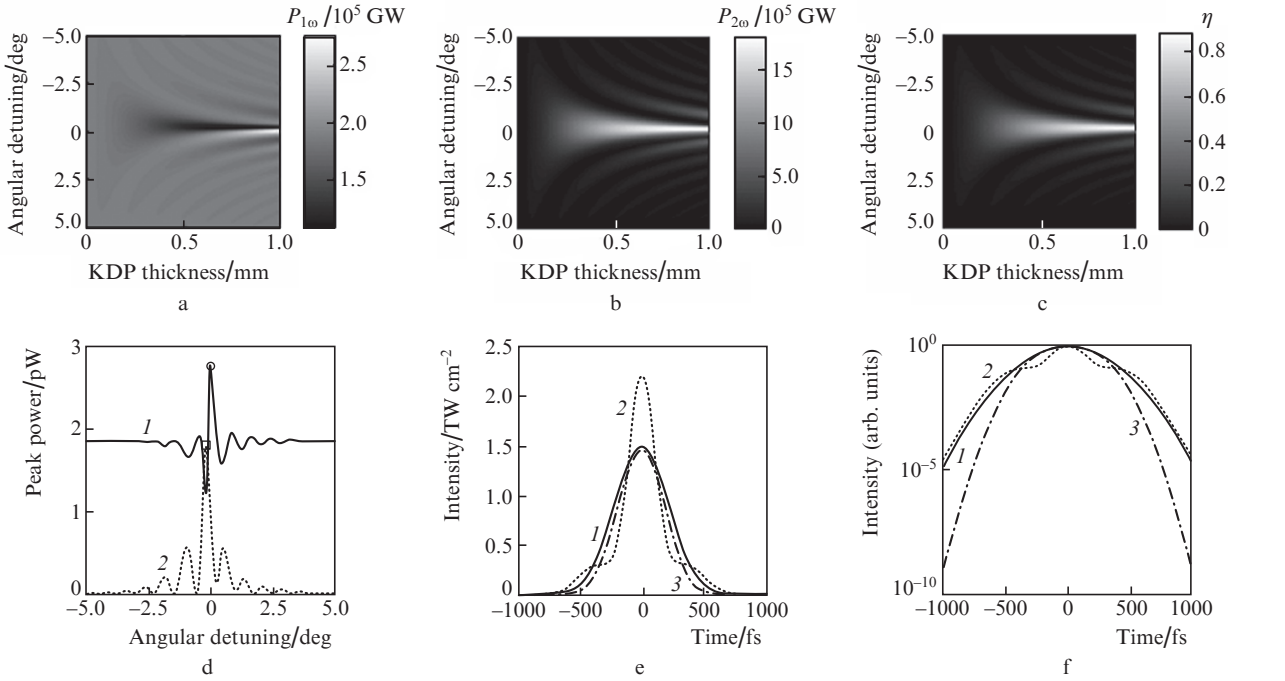


**Figure 3.** Second harmonic generation vs. angular detuning: peak intensity of (a) the first ($1\omega$) and (b) second ($2\omega$) harmonics as functions of the angular detuning and KDP thickness; (c) energy conversion efficiency $\eta$ as a function of the angular detuning and KDP thickness; (d) peak intensity of (*1*) the first and (*2*) second harmonics as functions of the angular detuning at the end of the crystal; temporal intensity profile of (*1*) the initial pulse, optimal (*2*) first (e) and (*3*) second (f) harmonics in linear (logarithmic) scale.

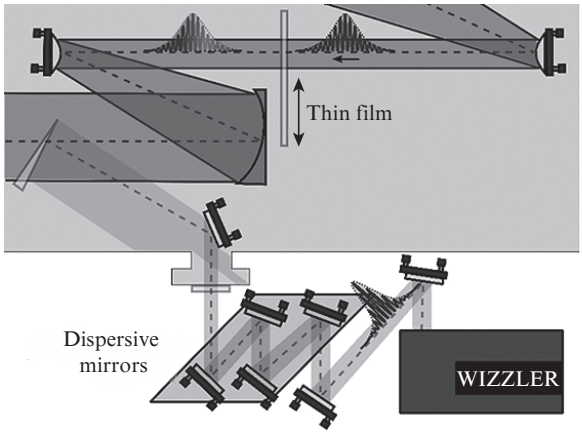


**Figure 4.** Experimental setup installed at the frontend of the petawatt CETAL laser facility with areas in gray denoting sections within the vacuum chamber. The beam is reduced in size to approximate the full propagation intensity of the petawatt beam. It is then expanded and attenuated through reflection before exiting vacuum for post-compression by the negative dispersive chirped mirrors during transport to the diagnostics instrumets.

controlling the nonlinear distortions of the pulse but also for protecting the transport optics from potential damage.

### 3.1. Methods

The diameter of the beam from the frontend of the petawatt CETAL laser is reduced from 65 mm to approximately 11 mm to achieve an energy density typical of unfocused petawatt pulses. To this end, use is made of spherical mirrors SM1 ($f$ = 500 mm) and SM2 ($f$ = –100 mm) before interaction with a 0.5-mm-thick film sample of cellulose acetate, followed by expansion by a similar telescope. After expansion the beam is attenuated by surface reflection from an uncoated wedge. The resulting pulse is re-compressed by negative-dispersion chirped mirror pairs place outside of a vacuum chamber. The spectral and temporal parameters of the pulses are measures using a combination of a USB spectrometer and a WIZZLER (Fastlite). These diagnostics measure the pulse's spectrum and relative spectral phase allowing for the reconstruction of the pulse temporal intensity profile from this information.

### 3.2. Results

The original pulse duration is measured with the thin film removed, and after recompression with three pairs of chirped mirrors ($\alpha$ = –40 fs$^2$ per bounce) it was 46 ± 2 fs. Figure 5a shows the resultant pulse spectra after interaction with 0.5-mm-thick films of cellulose acetate with increasing pulse energy. The measured spectral amplitude and phase for a pulse of intensity of 1.4 TW cm$^{-2}$ are shown in Fig. 5b both with and without the thin film. The reconstructed pulse intensity envelope is shown in Fig. 5c. The results of post-compression by combinations of chirped mirrors to compensate for the combination of the material interaction, dispersion within the vacuum window, and the transport through air to the measurement device are compared and the optimum compression (Fig. 5b) under the current conditions is achievable with a single pair of chirped mirrors that provided a GDD of –250 fs$^2$ per bounce. The pulse is compressed from approximately 46 ± 2 fs to 29 ± 1 fs. It was observed during the experi-

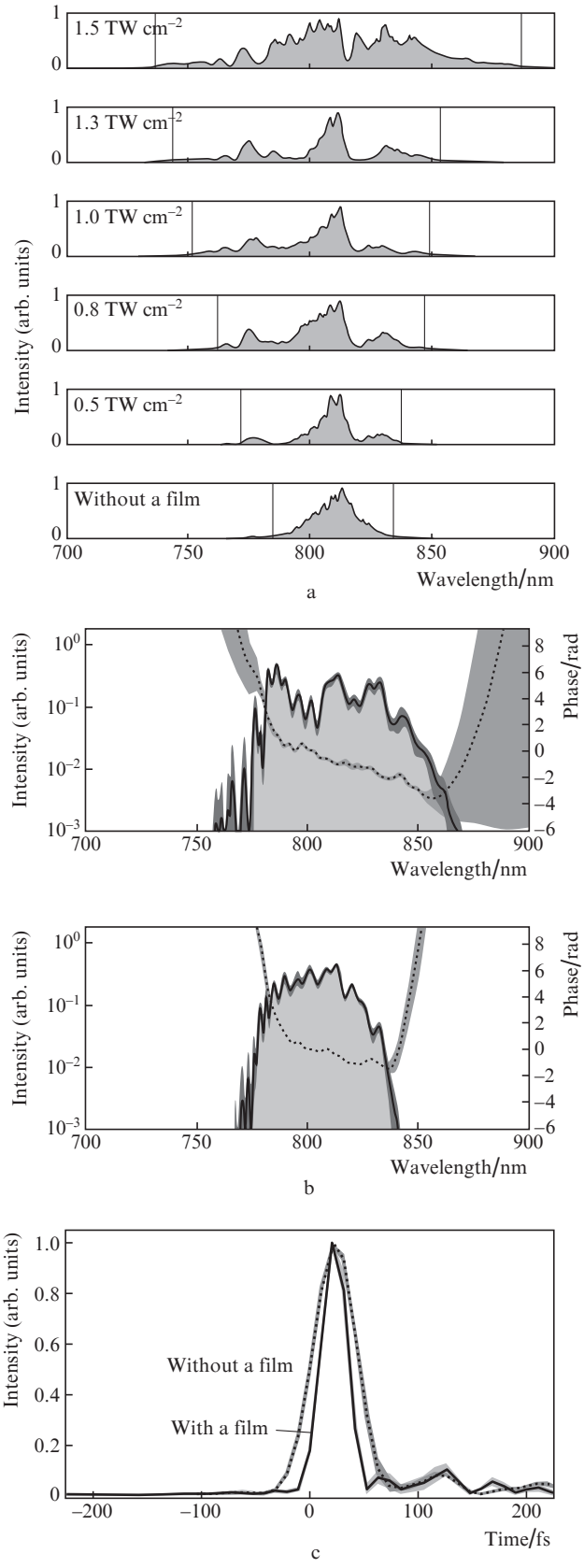


**Figure 5.** (a) Spectral broadening with increasing pulse intensity, (b) comparison of the spectral amplitude (solid curves) and phase (dashed curves) with (top) and without (bottom) a cellulose acetate film at an intensity of 1.4 TW cm$^{-2}$ and (c) reconstructed temporal intensities corresponding to the measured spectra.

ment that shorter pulses were achievable but the measurement seemed limited due to the condition of the initial beam and the bandwidth limit of the WIZZLER diagnostic unit. Also it should be noticed that the used cellulose acetate plane-parallel plate changed the beam profile insignificantly for the mentioned laser parameters.

## 4. Conclusions

We have considered three methods of additional pulse compression after the standard grating compressor: self-phase modulation and spectral phase correction by a chirped mirror, second harmonic generation and spectral phase correction by a chirped mirror, and cascaded quadratic nonlinearity that permits self-compression. The first method has been successfully tested at the petawatt CETAL laser facility. All three methods clearly demonstrate the possibility of enhancing the peak power of pulses delivered by modern high-energy petawatt laser facilities. These techniques can be applied with sufficient ease following the optical compressor at any types of powerful laser systems. This has great promise in extending the intensities that a laser facility might attain without requiring costly upgrades to the amplification chain.

***Acknowledgements.*** The work was supported by the Presidium of the Russian Academy of Science (Programme 'Extreme laser radiation: physics and fundamental applications') and the Ministry of Education and Science of the Russian Federation (Agreement No. 14.Z50.31.0007).

## References

1. Gaul E.W., Martinez M., Blakeney J., Jochmann A., Ringuette M., Hammond D., Borger T., Escamilla R., Douglas S., Henderson W., Dyer G., Erlandson A., Cross R., Caird J., Ebbers C., Ditmire T. *Appl. Opt.*, **49**, 1676 (2010).
2. Batani D., Koenig M., Miquel J.L., Ducret J.E., d'Humieres E., Hulin S., Caron J., Feugeas J.L., Nicolai P., Tikhonchuk V., Serani L., Blanchot N., Raffestin D., Thfoin-Lantuejoul I., Rosse B., Reverdin C., Duval A., Laniesse F., Chancé A., Dubreuil D., Gastineau B., Guillard J.C., Harrault F., Lebœuf D., Le Ster J.-M., Pès C., Toussaint J.-C., Leboeuf X., Lecherbourg L., Szabo C.I., Dubois J.-L., Lubrano-Lavaderci F. *Phys. Scr.*, **161**, 14016 (2014).
3. Blanchot N., Behar G., Berthier T., Bignon E., Boubault F., Chappuis C., Coïc H., Damiens-Dupont C., Ebrardt J., Gautheron Y., Gibert P., Hartmann O., Hugonnot E., Laborde F., Lebeaux D., Luce J., Montant S., Noailles S., Néauport J., Raffestin D., Remy B., Roques A., Sautarel F., Sautet M., Sauteret C., Rouyer C. *Plasma Phys. Control. Fusion*, **50**, 124045 (2008).
4. Yanovsky V., Chvykov V., Kalinchenko G., Rousseau P., Planchon T., Matsuoka T., Maksimchuk A., Nees J., Cheriaux G., Mourou G., Krushelnick K. *Opt. Express*, **16**, 2109 (2008).
5. Mével E., Tcherbakoff O., Salin F., Constant E.J. *Opt. Soc. Am. B*, **20**, 105 (2003).
6. Mourou G., Mironov S.Yu., Khazanov E.A., Sergeev A.M. *Eur. Phys. J. Spec. Top.*, **223**, 1181 (2014).
7. Agarwal G.P. *Nonlinear Fiber Optics* (San Diego: Acad. Press, 2006).
8. Ginzburg V.N., Kochetkov A.A., Yakovlev I.V., Mironov S.Yu., Shaykin A.A., Khazanov E.A. *Quantum Electron.*, **46**, 106 (2016) [*Kvantovaya Elektron.*, **46**, 106 (2016)].
9. Bespalov V.I., Talanov V.I. *Pis'ma Zh. Eksp. Teor. Fiz.*, **3**, 471 (1966) [*JETP Lett.*, **3**, 307 (1966)].
10. Mironov S., Lozhkarev V., Luchinin G., Shaykin A., Khazanov E. *Appl. Phys. B*, **113**, 147 (2013).
11. Mironov S.Y., Ginzburg V.N., Gacheva E.I., Silin D.E., Kochetkov A.A., Mamaev Y.A., Shaykin A.A., Khazanov E.A., Mourou G.A. *Laser Phys. Lett.*, **12**, 25301 (2015).
12. Lassonde P., Mironov S., Fourmaux S., Payeur S., Khazanov E., Sergeev A., Kieffer J.-C., Mourou G. *Laser Phys. Lett.*, **13**, 75401 (2016).
13. Akhmanov S.A., Chirkin A.S., Vysloukh V.A. *Optics of Femtosecond Pulses* (New York: AIP, 1991; Moscow: Nauka, 1988).
14. Razumikhina T.V., Telegin L.S., Kholodnykh A.I., Chirkin A.S. *Sov. J. Quantum Electron.*, **14**, 1358 (1984) [*Kvantovaya Elektron.*, **11**, 2026 (1984)].
15. Mironov S.Yu., Lozhkarev V.V., Ginzburg V.N., Yakovlev I.V., Luchinin G., Shaykin A., Khazanov E.A., Babin A., Novikov E., Fadeev S., Sergeev A.M., Mourou G.A. *IEEE J. Sel. Top. Quantum Electron.*, **18**, 7 (2012).
16. Liu X., Qian L., Wise F. *Opt. Lett.*, **24**, 1777 (1999).
17. Bache M., Bang O., Krolikowski W., Moses J., Wise F.W. *Opt. Express*, **16**, 3273 (2008).